Eur. Phys. J. D **33**, 323–327 (2005)
DOI: 10.1140/epjd/e2005-00047-3

THE EUROPEAN PHYSICAL JOURNAL D

Laser spectroscopic investigation of Ca atoms in liquid helium

Comparison between spectral properties for liquid helium-3 and helium-4

Y. Moriwaki[1,a] and N. Morita[2,b]

[1] Department of Physics, Toyama University, Gofuku, Toyama 930-8555, Japan
[2] Department of Molecular Structure, Institute for Molecular Science, Myodaiji, Okazaki 444-8585, Japan

Received 21 September 2004 / Received in final form 14 March 2005
Published online 19 April 2005 –

Abstract. Excitation and emission spectra of the $4s^2\,{}^1\mathrm{S}_0$ – $4s4p\,{}^1\mathrm{P}_1$ and $4s4p\,{}^3\mathrm{P}_J$ $(J = 0, 1, 2)$ – $4s5s\,{}^3\mathrm{S}_1$ transitions of Ca atoms implanted not only in liquid ^{4}He but also in liquid ^{3}He have been measured. It has been found that the excitation spectra for liquid ^{3}He show considerably smaller widths and peak shifts from transition wavelengths of a free Ca atom, in comparison with those for liquid ^{4}He. These spectral characteristics have been well reproduced by our theoretical calculation based on a vibrating bubble model. This calculation has shown that, due to a significant difference in surface tension between the two liquids, the radius of a bubble formed around Ca in liquid ^{3}He is larger than the one in ^{4}He, and that this fact as well as the smaller number density of He atoms in liquid ^{3}He cause weaker perturbation for Ca, resulting in the smaller peak shift and width for liquid ^{3}He.

PACS. 32.30.Jc Visible and ultraviolet spectra – 36.40.Mr Spectroscopy and geometrical structure of clusters – 67.40.Yv Impurities and other defects

1 Introduction

Recently, spectroscopic studies on impurity atoms and molecules in liquid helium have greatly been developed, and many authors have reported their interesting studies on diverse atomic and molecular species [1,2]. Those impurities in liquid helium usually reside in bubble-like cavities formed by Pauli's repulsive force between electrons in the impurities and in helium atoms. They are, therefore, affected by various perturbations from helium atoms surrounding them, and so their spectra significantly depend on physical properties of liquid helium. In particular, differences in physical properties between liquid ^{4}He (boson) and ^{3}He (fermion) may cause drastic differences in spectral characteristics of impurities. For example, Grebenev et al. have recently found sharp rotational spectral lines of OCS molecules in superfluid ^{4}He droplets, whereas only a broad peak in non-superfluid ^{3}He droplets [3]. From such a definite difference, they have interpreted the narrow rotational lines as an evidence of free rotation of the molecule and as a microscopic manifestation of superfluidity. This study shows that an impurity in liquid helium can be a micro-probe of quantum properties of liquid helium through laser spectroscopic techniques.

While the latter study demonstrates only a difference in the fluidity of liquid helium, there are some other differences in basic physical properties between liquid ^{3}He and ^{4}He, which are listed in Table 1. As seen in Table 1, not only the fluidity but the number density and surface tension also significantly differ between the two liquids, reflecting differences in mass and quantum statistics. It is interesting to investigate how these differences appear in spectral properties of impurities. For such investigations, not a molecule but an alkali atom or an alkali earth atom may, in general, be preferable as an impurity, because those atoms are known to form a simple bubble structure in liquid helium and so their spectra can more easily be analyzed; molecules are usually apt to attract He atoms strongly to form tight clusters around themselves.

Table 1. Physical properties of liquid ^{3}He and ^{4}He.

properties	helium-3	helium-4
mass (au)	3.0160	4.0026
nuclear spin	1/2	0
fluidity*	normal	super
density (cm^{-3})*	1.62×10^{22}	2.19×10^{22}
surface tension (dyn/cm)*,†	0.116	0.336

* values at a temperature of 1.4 K. † [5].

Based on these considerations, in the present work we have experimentally measured excitation and emission spectra of the $4s^2\,{}^1\mathrm{S}_0$ – $4s4p\,{}^1\mathrm{P}_1$ and $4s4p\,{}^3\mathrm{P}_J$ $(J = 0, 1, 2)$ – $4s5s\,{}^3\mathrm{S}_1$ transitions of Ca in liquid ^{3}He as well as in liquid ^{4}He. Although measurements of these transitions for liquid ^{4}He have already been reported [4],

[a] e-mail: moriwaki@sci.toyama-u.ac.jp
[b] *Present address*: Department of Applied Physics, Fukui University, Bunkyo, Fukui 910-8507, Japan.

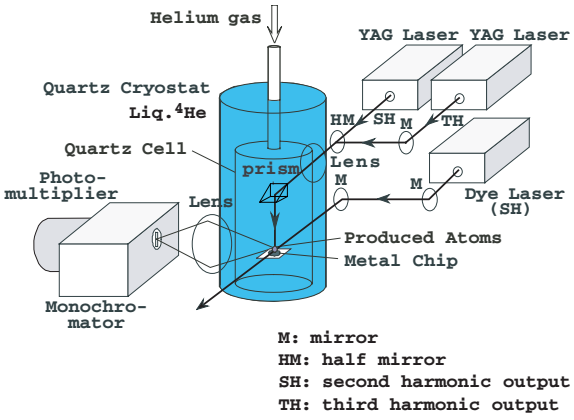

Fig. 1. Experimental setup.

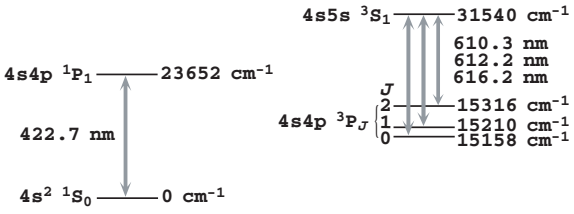

Fig. 2. Diagram of relevant energy levels in calcium atom. Transition wavelengths shown are those of a free Ca atom.

we have again measured them for detailed comparison with the spectra for liquid ^{3}He. In addition, to analyze the experimental spectra, we have also carried out theoretical calculations of the spectra. We will report these results in this paper.

2 Experimental

The experimental setup is shown in Figure 1. Helium-3 gas (99.95% in purity) or helium-4 gas (99.9999%) is introduced into a quartz cell, which is immersed into liquid ^{4}He kept at a temperature of 1.4 K, and the gas is gradually liquefied in the cell. Calcium atoms are implanted into the liquid He by laser sputtering of a Ca metal chip placed in the liquid He with two successive light pulses, which are second and third harmonic pulses of Nd^{3+}:YAG lasers, respectively; the width and energy of each pulse are 5 ns and 2 mJ, respectively. The Ca atoms thus produced are then excited by a dye laser pulse or its second harmonic pulse; the dyes used in the present observation are Coumarin 500, Fluorescane 548, Rhodamine 590(Chloride) and LDS 821. Laser induced fluorescence (LIF) from the atoms is introduced into a 25 cm monochromator through a lens and detected by a photomultiplier.

Relevant energy levels of Ca atom are diagrammatically shown in Figure 2. Excitation spectra are measured by scanning the dye laser wavelength with the monochromator wavelength fixed at each emission peak, while emission spectra are measured by scanning the monochromator wavelength with the laser wavelength fixed at each absorption peak.

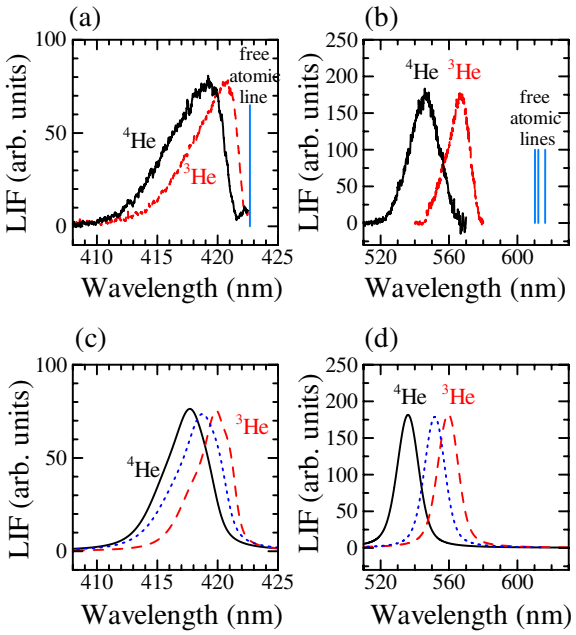

Fig. 3. Excitation spectra of Ca atoms in liquid ^{4}He (solid curves) and ^{3}He (dashed curves); (a) and (c) are experimental and theoretical spectra, respectively, for the $4s^2\ ^1S_0 \rightarrow 4s4p\ ^1P_1$ transition, and (b) and (d) experimental and theoretical spectra, respectively, for the $4s4p\ ^3P_J$ ($J = 0, 1$ and 2) $\rightarrow 4s5s\ ^3S_1$ transitions. Each vertical line indicates the transition wavelength in free space. The dotted curves in (c) and (d) indicate the result of a calculation for liquid ^{3}He, in which the surface tension is artificially changed to the same value as that for liquid ^{4}He.

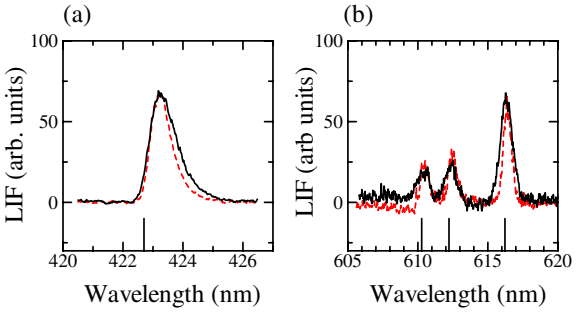

Fig. 4. Experimental emission spectra of Ca atoms in liquid ^{4}He (solid curves) and ^{3}He (dashed curves); (a) the $4s^2\ ^1S_0 \leftarrow 4s4p\ ^1P_1$ transition and (b) the $4s4p\ ^3P_J$ ($J = 0, 1$ and 2) $\leftarrow 4s5s\ ^3S_1$ transitions. Each vertical line indicates the transition wavelength in free space.

Excitation spectra observed for the $4s^2\ ^1S_0 - 4s4p\ ^1P_1$ and $4s4p\ ^3P_J (J = 1, 2, 3) - 4s5s\ ^3S_1$ transitions are shown in Figures 3a and 3b, respectively, and emission spectra observed for the same transitions are shown in Figure 4. As seen in Figures 3a and 3b, all the excitation spectra show broad widths and large blue shifts of the peak positions from the transition wavelengths in free space. These are usual spectral characteristics for impurity atoms in liquid He. However, we can clearly see large isotopic differences in those spectral properties between liquid ^{3}He

Table 2. Spectral properties obtained in the present measurements.

transitions	liquid	peak position shift (nm)	spectral width (nm)
$4s^2\ ^1S_0 \rightarrow 4s4p\ ^1P_1$	^{3}He	–2.0 ± 0.1	4.4 ± 0.2
	^{4}He	–3.5 ± 0.1	5.3 ± 0.2
$4s4p\ ^3P_0 \rightarrow 4s5s\ ^3S_1$	^{3}He	–43.5 ± 1	15.1 ± 1
	^{4}He	–64 ± 1	21.1 ± 1
$4s^2\ ^1S_0 \leftarrow 4s4p\ ^1P_1$	^{3}He	0.5 ± 0.1	0.8 ± 0.1
	^{4}He	0.5 ± 0.1	1.1 ± 0.1
$4s4p\ ^3P_0 \leftarrow 4s5s\ ^3S_1$	^{3}He	0.2 ± 0.1	0.7 ± 0.1
	^{4}He	0.2 ± 0.1	1.1 ± 0.1
$4s4p\ ^3P_1 \leftarrow 4s5s\ ^3S_1$	^{3}He	0.3 ± 0.1	0.7 ± 0.2
	^{4}He	0.3 ± 0.1	1.0 ± 0.2
$4s4p\ ^3P_2 \leftarrow 4s5s\ ^3S_1$	^{3}He	0.3 ± 0.1	0.7 ± 0.2
	^{4}He	0.2 ± 0.1	1.0 ± 0.2

and ^{4}He; that is, the spectral widths for liquid ^{3}He are considerably narrower than those for liquid ^{4}He, and the blue peak shifts for ^{3}He are significantly smaller than those for ^{4}He. On the other hand, as seen in Figure 4, the emission spectra also show similar isotopic differences in spectral widths and peak shifts, although the peak shifts are at the red side in turn, as usual for emission spectra of impurity atoms. However, the widths and peak shifts of these emission spectra are very small, and so their isotopic differences are much less clear than the ones in the excitation spectra. Quantitative properties of all these spectra are summarized in Table 2.

3 Theoretical calculations of the spectra

To understand the above characteristic properties of the experimental spectra, we have carried out model calculations to obtain theoretical spectra on the basis of a bubble model, in which a bubble-like structure for He atoms surrounding a Ca atom is assumed. In the emission spectra, as seen in Figure 4, the peak shifts and spectral widths are both quite small, so that their differences between liquid ^{3}He and ^{4}He are also very small and almost comparable to the present experimental ambiguity. This means that, even if their theoretical spectra are calculated, we cannot expect meaningful discussions. Therefore, in the present calculation we have concentrated only on the excitation spectra.

The formulation of the bubble model are summarized by Kanorsky and Weis [6] and Tabbert et al. [7]. The procedure of the present model calculation based on this formulation is almost the same as has already been published [8], and in brief as follows.

First, we assume that the density profile of He atoms around an impurity atom is expressed in the form

$$\rho(r) = \begin{cases} \rho_0 \{1 - [1 + \alpha(r - r_0)] \exp[-\alpha(r - r_0)]\}, & \text{for } r > r_0, \\ 0, & \text{for } r < r_0, \end{cases} \quad (1)$$

where ρ_0 is the number density of helium atoms in the normal region, which is described by physical parameters given in Table 1, and r_0 and α are parameters representing the size of the bubble and the slope of the He number density at the bubble interface, respectively.

For a vibrating bubble, r_0 is a function of the solid angle Ω:

$$r_0 = r_e + \sum_{\substack{\lambda = 0, 1, 2, \ldots \\ \mu = 0, 1, 2, \ldots, \lambda \\ \nu = \begin{cases} \pm \text{ (for } \mu \neq 0) \\ + \text{ (for } \mu = 0) \end{cases}}} a_{\lambda\mu\nu} Y'_{\lambda\mu\nu}(\Omega), \quad (2)$$

where

$$Y'_{\lambda\mu+}(\Omega) = \begin{cases} \sqrt{2}\ \mathrm{Re}\ Y_{\lambda\mu}(\Omega), & \text{for } \mu \neq 0, \\ Y_{\lambda 0}(\Omega), & \text{for } \mu = 0, \end{cases} \quad (3)$$

$$Y'_{\lambda\mu-}(\Omega) = \sqrt{2}\ \mathrm{Im}\ Y_{\lambda\mu}(\Omega), \qquad \text{for } \mu \neq 0, \quad (4)$$

and $Y_{lm}(\Omega)$ is the spherical harmonic function. The terms with $\lambda = 0$, 1, 2, ... in equation (2) represent the bubble vibrations in the spherical mode (breathing mode), dipole mode, quadrupole mode, and so on, respectively, and $a_{\lambda\mu\nu}$ is the vibration amplitude in each mode.

Here we note that, for calculations on the number density profile in liquid ^{3}He, we should discuss the existence of ^{4}He atoms as impurities, like the case of an OCS-He system in reference [3]. The potential well depth of a Ca−He pair in each relevant state is too shallow for a ^{4}He atom to couple tightly with a Ca atom [9]. The difference of the (zero-point) vibrational energy between Ca−^{3}He and Ca−^{4}He pairs is much smaller than the liquid temperature (1.4 K). These facts mean that the thermal fluctuation prevents ^{4}He atoms from clustering around Ca atoms in liquid ^{3}He. We can thus assume a uniform distribution of ^{4}He atoms in liquid ^{3}He, and finally neglect the ^{4}He atoms because of their small abundance ratio (0.05%).

The Hamiltonian of a Ca atom in liquid helium is given by

$$H = E_l + A_{LS} \boldsymbol{L} \cdot \boldsymbol{S} + H_{int} + E_c, \quad (5)$$

where E_l is the atomic energy excluding the spin-orbit coupling, A_{LS} the spin-orbit coupling constant, H_{int} the interaction energy between Ca and surrounding He atoms, and E_c the bubble cavity energy consisting of the surface energy, pressure volume work and volume kinetic energy of the bubble [10].

In the first-order approximation, the interaction Hamiltonian H_{int} is described by the sum of the potential energies of all Ca−He pairs, and is given by [6]

$${}^{2S+1}H^s_{int} = \int dV \rho(\boldsymbol{r})\, {}^{2S+1}V^s_\Sigma(r), \quad (6)$$

for the $4s^2\ ^1S_0$ and $4s5s\ ^3S_1$ states of Ca and

$${}^{2S+1}H^p_{int} = \int dV \rho(\boldsymbol{r}) \left\{ {}^{2S+1}V^p_\Sigma(r) + \left(\frac{\boldsymbol{L} \cdot \boldsymbol{r}}{\hbar r}\right)^2 [{}^{2S+1}V^p_\Pi(r) - {}^{2S+1}V^p_\Sigma(r)] \right\}, \quad (7)$$

Table 3. Bubble interface parameters determined to minimize the bubble energy.

state	liquid	r_0 (au)	α (/au)	r_b (au)
$4s^2\ ^1S_0$	^{4}He	9.26	1.16	11.1
	^{3}He	9.26	0.941	11.6
$4s4p\ ^3P_0$	^{4}He	10.30	1.18	12.1
	^{3}He	10.27	0.955	12.5

for the $4s4p\ ^1P_1$ and $4s4p\ ^3P_J$ ($J = 0$, 1 and 2) states. Here, $^{2S+1}V^L_\Sigma(r)$ and $^{2S+1}V^L_\Pi(r)$, in which $L = s$ or p, represent the potential energies of an Ca−He pair in its molecular states indicated by the subscripts, the superscripts s and p indicate the $^{2S+1}S_J$ and $^{2S+1}P_J$ states of the Ca atom, respectively, and the superscript $2S + 1$ indicates the spin multiplicity. These potential energies at each r are given by adiabatic potential curves calculated by Czuchaj et al. [9].

Our calculation procedure to obtain theoretical spectra from the above equations is, in principle, as follows: first, eigenvalue problems of the Hamiltonian H are solved to obtain adiabatic potential surfaces for both initial and final bubble states, as functions of the vibration amplitudes $a_{\lambda\mu\nu}$. Next, a vibrational wavefunction in the initial bubble state is calculated from its potential surface. Then, we calculate the time evolution of this wavefunction after transferred onto the potential surface of the final bubble state through an optical transition. Finally, calculating an autocorrelation function of this time evolution, we obtain the spectrum by the Fourier transform of the autocorrelation function. This procedure is called the "spectral method" [11], which is also used in our previous studies on Mg [12] and Yb^+ [8] in liquid helium.

3.1 Excitation spectrum of the $4s^2\ ^1S_0 - 4s4p\ ^1P_1$ transition

For the spherical $4s^2\ ^1S_0$ state, due to equation (6), the bubble is also spherical in the equilibrium state. The bubble interface parameters r_0 and α are determined to minimize the bubble energy. With these parameters, we can define an effective bubble radius r_b by the following equation: $\int_0^{r_b} \rho(r)4\pi r^2 dr = \int_{r_b}^{\infty}\{\rho_0 - \rho(r)\}4\pi r^2 dr$ [13]. The values thus determined for r_0, α and r_b are shown in Table 3. As seen in Table 3, the parameter α for liquid ^{3}He is smaller by about 20% than the one for liquid ^{4}He, while r_0 is almost the same for both the liquids. These facts result in a larger effective bubble radius r_b for liquid ^{3}He, as seen in Table 3.

In this calculation, we take into consideration the bubble vibration in the lowest three modes ($\lambda = 0$, 1 and 2 in Eq. (1)); the spherical breathing mode, the dipole mode and the quadrupole mode. When a Ca atom in the ground state is excited into the $4s4p\ ^1P_1$ state, the energy level is split into two levels for the dipole vibration mode and into three levels for the quadrupole mode, due to the anisotropy of the interaction potential between a Ca atom and a bubble. This causes the spectral broadening just similar to the D2 excitation in alkali atoms and alkali earth ions, for which even spectral splittings are sometimes observed [8,14]. Consequently, we obtain such a theoretical spectrum as shown in Figure 3c.

3.2 Excitation spectra of the $4s4p\ ^3P_J - 4s5s\ ^3S_1$ transitions

The $4s4p\,^3P_J$ ($J = 0, 1$ and 2) states are metastable states, the lifetime of which is 0.4 ms for the $J = 1$ state and much longer for the $J = 0$ and 2 states [15]. These lifetimes are long enough to observe the $4s4p\,^3P_J - 4s5s\ ^3S_1$ transitions with an excitation laser pulse 50 μs after the second sputtering laser pulse. Considering the Boltzmann distribution for these triplet levels, we can see that almost all of the population is in the lowest $J = 0$ state, because the temperature (1.4 K) of the liquid helium is very low compared with the separation between each adjacent triplet level (52 and 106 cm^{-1}). This means that it is sufficient to take into consideration only the $4s4p\,^3P_0$ state as the initial state in the calculation of the spectra.

As can be seen from equation (7), the interaction potential between Ca in the $4s4p\,^3P_0$ state and He atoms is spherical. The bubble interface parameters determined for this state are given in Table 3. As seen in Table 3, the slope α of the number density at the bubble interface in liquid ^{3}He is smaller than the one in liquid ^{4}He, and so the effective bubble radius r_b in liquid ^{3}He is larger than the one in liquid ^{4}He. These characteristics are just the same as in the $4s^2\,^1S_0$ state.

Also in this calculation, the lowest three modes of the bubble surface vibration are taken into consideration. Since the upper state ($4s5s\ ^3S_1$) is also spherical, vibrational potential surfaces for the dipole and quadrupole modes are both spherical. Therefore, unlike $4s4p\ ^1P_1$, the $4s5s\ ^3S_1$ state is not split by either the dipole or quadrupole mode vibration, and this fact results in narrower spectra. The calculated spectra are shown in Figure 3d.

4 Discussions

As seen in Figure 3, the experimental excitation spectra are considerably well reproduced by the theoretical calculations. Although absolute values of the peak wavelength and spectral width calculated for each transition slightly differ from the experimental values, relative differences in peak shift and spectral width between liquid ^{3}He and ^{4}He are well reproduced by the calculations; both in the experimental and theoretical results, the peak shifts for liquid ^{3}He are smaller than the ones for liquid ^{4}He by about 40 and 30% for the $4s^2\ ^1S_0 - 4s4p\ ^1P_1$ and $4s4p\,^3P_0 - 4s5s\ ^3S_1$ transitions, respectively, and the spectral width for ^{3}He is smaller than the one for ^{4}He by about 18% for the $4s^2\ ^1S_0 - 4s4p\ ^1P_1$ transition (only the calculated isotopic difference in the spectral width for the

$4s4p\ ^3\mathrm{P}_0 - 4s5s\ ^3\mathrm{S}_1$ transition is exceptional and quite small compared with the experimental difference). This result allows us to infer that our model calculations appropriately include the basic origin of the large spectral differences experimentally observed between liquid ^{3}He and ^{4}He.

Smaller peak shifts and spectral widths in the excitation spectra for liquid ^{3}He indicate that the perturbation for the valence electron of a Ca atom by surrounding ^{3}He atoms is smaller than the one caused by ^{4}He atoms. There are, however, no significant differences between the Ca−^{3}He and Ca−^{4}He interaction potentials. One of the possible reasons for such weaker perturbation in liquid ^{3}He is the smaller number density of He atoms. In fact, as seen in Table 1, the He number density in liquid ^{3}He is quite small compared with the one in liquid ^{4}He. This is mainly due to the smaller mass of ^{3}He; that is, the wave function of a ^{3}He atom having smaller mass spreads to an extent larger than ^{4}He, and this causes a longer average distance between each ^{3}He atom. It is reasonable that such lower He number density results in weaker total perturbations for Ca atoms in liquid ^{3}He.

Moreover, as shown in Table 3, the slope α of the He number density at the bubble interface in liquid ^{3}He is considerably smaller (soft cage), and consequently the effective bubble radius r_b in liquid ^{3}He is larger than the one in liquid ^{4}He. These facts result from the difference in surface tension; the surface tension of liquid ^{3}He is much smaller than that of liquid ^{4}He, being as small as one third of the latter at 1.4 K, as seen in Table 1, and this is mainly due to the quantum statistical difference between ^{3}He (fermion) and ^{4}He (boson). Such a larger and softer bubble in liquid ^{3}He should also reduce the perturbation for Ca atoms.

A test calculation is carried out by artificially changing the value of the surface tension so as to examine its effect on spectra. The dotted curves in Figures 3c and 3d indicate the result of the calculation for liquid ^{3}He, where the surface tension is changed to the same value as that for liquid ^{4}He, whereas the other parameters are left as the same values as those for liquid ^{3}He. It is found that for the $4s4p\ ^3\mathrm{P}_J \rightarrow 4s5s\ ^3\mathrm{S}_1$ transition, where a large amount of helium is transferred, the isotopic difference in spectra comes mainly from the density effect. But for the $4s^2\ ^1\mathrm{S}_0 \rightarrow 4s4p\ ^1\mathrm{P}_1$ transition, where helium transfer is considerably small, contribution by the effect of the surface tension is comparable to that of the density.

Consequently, as long as one assumes the bubble model, it may be reasonable to conclude that the large spectral differences between liquid ^{3}He and ^{4}He are basically caused by differences in number density of He atoms and in bubble size. The latter differences are originated from differences in mass and in quantum statistics between the two isotopic species of He. Therefore, the present results may be interpreted as microscopic manifestations of differences in basic physical properties between ^{3}He and ^{4}He.

5 Conclusion

We have experimentally observed excitation and emission spectra of the $4s^2\,^1\mathrm{S}_0 - 4s4p\ ^1\mathrm{P}_1$ and $4s4p\,^3\mathrm{P}_J$ ($J = 0, 1, 2$) $- 4s5s\ ^3\mathrm{S}_1$ transitions of Ca atoms in liquid ^{3}He as well as in liquid ^{4}He, and have found that there are significant spectral differences between the excitation spectra in liquid ^{3}He and ^{4}He; that is, their peak shifts and spectral widths for liquid ^{3}He are both much smaller than those for liquid ^{4}He. In order to clarify the cause for these isotopic differences of the spectra, we have also carried out theoretical calculations based on a bubble model including bubble surface vibrations up to the quadrupole mode, and have found that the theoretical spectra thus calculated considerably well reproduce the differences seen in the experimental spectra. The calculations have shown that, due to a significant difference in surface tension between liquid ^{3}He and ^{4}He, the radius of a bubble formed around Ca in liquid ^{3}He is larger than the one in ^{4}He. Consequently, we have concluded that this fact as well as the smaller number density of He atoms in liquid ^{3}He cause weaker perturbation for Ca, resulting in the smaller peak shift and width in the spectra for liquid ^{3}He.

This work was partly supported by a Grant-in-Aid for Scientific Research from the Ministry of Education, Science, Sports, and Culture.

References

1. S.I. Kanorsky, A. Weis, Adv. At. Mol. Opt. Phys. **38**, 87 (1998)
2. *Helium Nanodroplets: A Novel Medium for Chemistry and Physics*, edited by B. Whaley, R. Miller, J. Chem. Phys. **115**, No. 22 (2001)
3. S. Grebenev, J.P. Toennies, A.F. Vilesov, Science **279**, 2083 (1998)
4. H. Bauer, M. Beau, A. Bernhardt, B. Friedl, H.J. Reyher, Phys. Lett. A **137**, 217 (1989)
5. M. Iino, M. Suzuki, A.J. Ikushima, J. Low Temp. Phys. **61**, 155 (1985)
6. S.I. Kanorsky, A. Weis, *Atoms in nanocavities*, edited by M. Ducloy, D. Bloch, *Quantum Optics of Confined Systems* (Kluwer Academic, Netherlands, 1996), pp. 367-393
7. B. Tabbert, H. Günther, G.zu Putlitz, J. Low Temp. Phys. **109**, 653 (1997)
8. Y. Moriwaki, N. Morita, Eur. Phys. J. D **13**, 11 (2001)
9. E. Czuchaj, F. Rebentrost, H. Stoll, H. Preuss, Chem. Phys. Lett. **182**, 191 (1991)
10. K. Hiroike, N.R. Kestner, S.A. Rice, J. Jortner, J. Chem. Phys. **43**, 2625 (1965)
11. M.D. Feit, J.A. Fleck Jr, A. Steiger, J. Comput. Phys. **47**, 412 (1982)
12. Y. Moriwaki, N. Morita, Eur. Phys. J. D **5**, 53 (1999)
13. A.P. Hickman, W. Steets, N.F. Lane, Phys. Rev. B **12**, 3705 (1975)
14. T. Kinoshita, K. Fukuda, T. Yabuzaki, Phys. Rev. B **54**, 6600 (1996)
15. A.A. Radzig, B.M. Smirnov, *Reference data on atoms, molecules, and ions* (Springer-Verlag, Berlin, 1985)